Optics Letters

Parametric amplification in large-aperture diffusion-bonded periodically poled crystals

Eli Sobolev,[1] Pavel Komm,[1] Salman Noah,[2] and Gilad Marcus[1,*]

[1]Department of Applied Physics, Faculty of Mathematics and Sciences, The Hebrew University of Jerusalem, 91904, Jerusalem, Israel
[2]Department of Applied Physics, Electro-Optics Engineering Faculty, Jerusalem College of Technology, Havaad Haleumi 21, Jerusalem, Israel
*Corresponding author: gilad.marcus@mail.huji.ac.il

Received 8 January 2019; revised 28 January 2019; accepted 1 February 2019; posted 4 February 2019 (Doc. ID 357109); published 1 March 2019

With conventional poling techniques of pyroelectric crystals, the thickness of the periodically poled crystals is typically limited to 0.5–1 mm. Such a small aperture of the crystal limits the amount of energy/power that this device may deliver. Here we discuss diffusion bonding as an alternative method to achieve a wider periodically poled crystal, with virtually unlimited width. It is shown that the amplified signal preserved a good beam profile despite a possible phase shift between the stitched crystals. This technique may be extended to larger aperture optical parametric amplifiers and allows for high energy output from periodically poled crystals.

https://doi.org/10.1364/OL.44.001261

Optical parametric amplification (OPA) is a process in which a strong pump field nonlinearly interacts with a medium to drive secondary waves at different frequencies. In the most common case, where the interacting medium has a noncentrosymmetric structure, the pump wave at frequency ω_p either generates or amplifies two additional waves, termed the signal and the idler waves at frequencies ω_s and ω_i, where energy conservation imposes $\omega_p = \omega_s + \omega_i$ [1]. Besides the mandatory condition of energy conservation, maximum gain will be obtained when the phase-matching condition $\Delta k = k_s + k_i - k_p = 0$ is satisfied; here, k_p, k_s, and k_i are the wave vectors of the interacting pump, signal, and idler beams, respectively [2].

Usually, it is difficult to achieve phase-matching conditions in an isotropic medium due to the characteristic dependence of the refractive index on wavelength. The most widespread approach to achieve phase-matching conditions is to use the different dispersions of the ordinary and extraordinary rays in birefringence materials. However, sometimes, even with birefringence materials, it is impossible to have phase-matching conditions. Quasi-phase matching (QPM), first proposed by Armstrong *et al.* [3], provides an extra variable to adjust and tailor phase-matching conditions for the desired wavelengths and the nonlinear medium. In QPM, the effective nonlinear coefficient of the medium is periodically modulated with modulation period Λ. The interacting waves in the periodically poled crystal have to satisfy the modified momentum and energy relations,

$$\Delta k_Q = k_s + k_i - k_p \pm \frac{2\pi}{\Lambda} = 0, \tag{1}$$

$$\hbar\omega_p = \hbar\omega_s + \hbar\omega_i, \tag{2}$$

where Δk_Q is the quasi-phase mismatch. When $\Delta k_Q = 0$, the system is in the phase-matching condition. At present, the most extensively applied method for implementing QPM is electric field poling of ferroelectric oxide crystals [4].

QPM plays an important role in many applications, including frequency doubling [5], optical parametric oscillators [6], optical parametric generators [7,8], and optical parametric amplifiers [2,9,10]. In the context of optical parametric amplifiers, a major goal is to extract high output power/high output pulse energy. In this context, one of the main problems with OPAs, based on periodically poled crystals, is their small aperture.

With mature periodic poling techniques, the thickness of the periodically poled crystal is typically limited to 0.5–1 mm [11,12], and there is a continuous effort to increase their thickness. A noncommercial 5 mm thick periodically poled Rb-doped $KTiOPO_4$ (KTP) crystal structure [11] and a 3 mm thick periodically poled structure of isomorphic $RbTiOAsO_4$ (RTA) crystals [13] have been reported. RTA shows a considerably lower ionic conductivity compared to KTP, which can be used for large-aperture poling [11], but this material is not commercially available. Lithium niobate ($LiNbO_3$, LN) and lithium tantalate ($LiTaO_3$, LT) are the most widely explored ferroelectric families for periodically poled crystals [4] due to their relatively high nonlinearity (LN has the largest d33 coefficient of 28 pm/V while LT has 16 pm/V [4]), a wide transparency range from UV to mid-IR [14,15], and commercial availability. It was shown that by doping these crystals with magnesium, it is possible to achieve a higher damage threshold and a lower coercive field [16], which makes it possible to use larger cross-section crystals in the poling process. Near-stoichiometric LN and LT (SLN and SLT) crystals have a wide transparency range and large electro- and nonlinear-optic coefficients compared to congruent crystals [17]. It has been reported that SLT has a lower coercive field and a higher photorefractive damage threshold than SLN, and is transparent up to

5 μm. Thus, it has been put forward as a promising candidate for high power and frequency downconversion devices [18]. A 5 mm × 5 mm aperture PPMgLN crystal [19] was used by Gu *et al.* [9] to deliver 714 μJ, 15.7 fs pulses at 2.1 μm. In a paper by Ishizuki and Taira [16], a high-energy optical parametric oscillation (OPO) using 5 mm thick PPMgLT was demonstrated and produced up to 118 mJ output using 196 mJ pumping with ~70% slope efficiency. Also, 10 mm thick PPMgLN was reported by Ishizuki [20].

In the present study, we discuss diffusion bonding as an alternative method to achieve a wider periodically poled crystal. We demonstrate it for stitching two crystals together, but this method could apply for stitching many crystals together, allowing for virtually unlimited crystal aperture. Direct bonding of two bulk $KTiPO_4$ (KTP) crystals was first applied by Tei *et al.* [21]. One joule of second-harmonic pulses with a repetition rate of 100 Hz was obtained by a 2.1 J pump beam. The authors observed a slight deterioration in the beam quality caused by the deformation of the crystal, but the obtained conversion efficiency was similar to that of a single bulk KTP crystal. Missey *et al.* described a 3 mm thick diffusion-bonded stack of periodically poled $LiNbO_3$ (PPLN) [22]. The increased aperture in their QPM-based OPO setup allowed them to use about 30 mJ pump power to obtain a 2 mJ signal beam at a pump energy of 22 mJ. Numerical simulation carried out by Michaeli *et al.* [12] examined the second-harmonic generated beam from two combined PPKTP crystals, one above the other with a phase difference in the polarization space. Both Missey *et al.* [22] and Michaeli *et al.* [12] concluded that a cardinal drawback of the diffusion-bonding technique, when used with periodically poled crystals, was its high sensitivity to the alignment of the poled domains between the stitched crystals (see Fig. 1), which may result in an asymmetric beam, even when a perfectly symmetric pump beam is employed.

In the current research, we show that when both the pump and signal have predetermined phases, i.e., they are real fields and not emerging from noise, it is possible to achieve a symmetrical amplified beam profile when it passes through the stitching interface between the two diffusion-bonded crystals.

The three-wave difference frequency mixing process is described by the three coupled equations given below [2]:

$$\frac{dA_i}{dy} = -i\frac{\omega_i}{n_i c} d_{\text{eff}} A_s^* A_p \exp(-i\Delta\phi), \tag{3a}$$

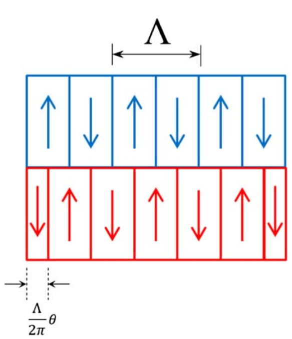

Fig. 1. Structure of the two diffusion-bonded periodically poled crystals.

$$\frac{dA_s}{dy} = -i\frac{\omega_s}{n_s c} d_{\text{eff}} A_i^* A_p \exp(-i\Delta\phi), \tag{3b}$$

$$\frac{dA_p}{dy} = -i\frac{\omega_p}{n_p c} d_{\text{eff}} A_s A_i \exp(i\Delta\phi), \tag{3c}$$

where all beams are propagating in the y direction; A_p, A_s, and A_i are the field amplitudes of the pump signal and idler, respectively; d_{eff} is the so-called effective nonlinear coefficient; and $\omega_p, \omega_s, \omega_i$ and n_p, n_s, n_i are the angular frequency and refractive indices of the pump, signal, and idler, respectively, with c being the speed of light in a vacuum. Finally, $\Delta\phi = \phi_i + \phi_s - \phi_p = (k_i + k_s - k_p)y$. From these equations, when $\Delta\phi$ is equal to zero, the oscillating factor in Eqs. (3a)–(3c) vanishes, and the conversion efficiency is maximized, leading to the above-mentioned phase-matching condition $\Delta k = k_i + k_s - k_p = 0$. In cases where this phase-matching condition cannot be met, it is possible to modulate the effective nonlinear coefficient such that $d_{\text{eff}} \to D_{\text{eff}} \exp(\pm i(\frac{2\pi}{\Lambda}y + \theta))$ [23], and the phase-matching condition can turn to the more general QPM condition,

$$\left(\phi_s + \phi_i - \phi_p \pm \theta \pm \frac{2\pi}{\Lambda}y\right) = 0. \tag{4}$$

The additional phase θ in the effective nonlinear coefficient is usually set to zero by choosing the proper origins of coordinates. However, when stitching two periodically poled crystals together, it is possible to have a residual phase θ due to some misalignment of the domains (see Fig. 1). This additional phase between the two halves of the beam could be a source for beam distortion and beam profile degradation as discussed also by Michaeli *et al.* [12]. Here we claim that this concern applies for applications in which only the phase of the pump beam is well defined, such as OPO, optical parametric generation (OPG), or in the case of second-harmonic generation, where the signal and idler phases are well defined, and the pump receives the residual phase. Equation (4) imposes the relationship between the phases of the three interacting fields; thus, if only the pump phase ϕ_p is predetermined, the two other phases could take any value [24]. However, in OPA applications, a pump beam with a well-defined phase is amplifying another signal beam, also with a well-defined phase. In such a case, we predict that the idler will take the residual phase. Therefore, in cases where there is a residual phase θ between the two stitched parts of the crystal, the beam profile of the amplified signal beam will remain symmetrical, and any possible beam distortion due to this additional phase will be directed to the idler beam.

To demonstrate the effect of the additional phase on the idler beam profile, we made some numerical simulations. The numerical simulation is based on a Fresnel diffraction integral that propagates a Gaussian beam with a phase between its two halves to a distance that is much larger than the Rayleigh range. The resulted beam profile is a perfect Gaussian when there is no phase difference ($\theta = 0$), and the two lobes appear with different phase differences (see Fig. 2). Similar profiles were predicted by Michaeli *et al.* [12] for a second-harmonic beam that is generated in a stitched periodically poled crystal.

Here we show experimentally the ability to parametrically amplify a signal beam in a large-aperture periodically poled

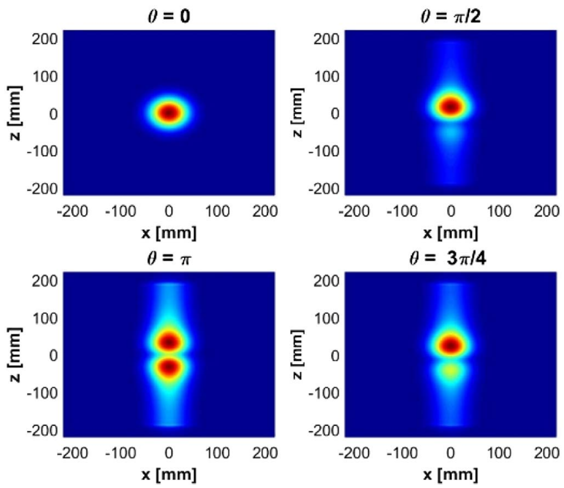

Fig. 2. Results from our numerical simulation, which demonstrates the effect of a phase θ between the two halves of a Gaussian beam. It shows the expected intensity distribution of the generated idler in the diffusion-bonded crystal under different domain misalignment between the two crystals.

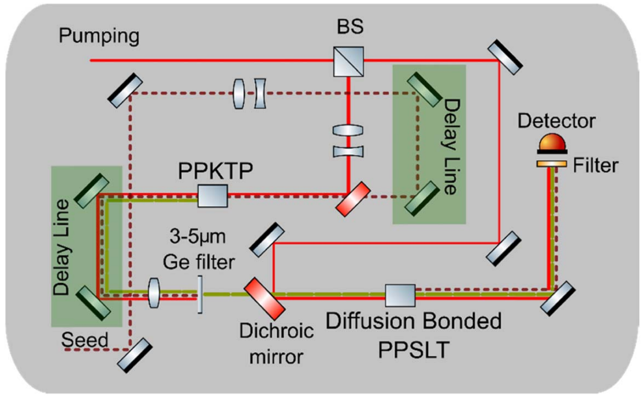

Fig. 3. Layout of the two OPCPA stages of the system. BS stands for beam splitter. The red lines represent the pumping paths, and the dashed brown lines represent the 1043 nm signal, which is used as a seed to create the mid-IR idler, drawn in the solid green line.

crystal, which is composed of two bonded periodically poled stoichiometric lithium tantalate (PPSLT) crystals with the same periodicity. The two crystals, each with initial sizes of 2.95 mm H × 9.53 mm W × 4.5 mm L, were diffusion-bonded together by Onyx Optics Inc. to form a stitched crystal with a size of 5.52 mm H × 9.53 mm W × 4.44 mm L (H, W, and L stand for high, width, and length, respectively). In our experiments, a two-stage optical parametric chirped pulse amplifier (OPCPA) pumped by a Ti:sapphire laser was utilized.

A very broadband Ti:sapphire oscillator with a central wavelength at 800 nm is the front end for the entire system. It was used to both seed a Ti:sapphire amplifier and the Yb-doped fiber amplifier. A small portion from the Ti:sapphire oscillator spectrum at the central wavelength of 1043 nm, with a bandwidth of 0.1 nm, was filtered and amplified by an ytterbium-doped fiber amplifier to further being used as the described signal seed. The central part of the Ti:sapphire spectrum (790–830 nm) was amplified using Ti:sapphire regenerative amplifier. The 1 kHz, 16 ps stretched pulse from the regenerative Ti:sapphire amplifier, centered at wavelength 815 nm, was used as a pump for our two-stage OPCPA. Figure 3 shows the experimental setup of the two OPCPA stages. For the first stage of the OPCPA system, a 7 mm long uncoated periodically poled potassium titanyl phosphate (PPKTP) was used, with a poling period of 27.1 μm. The PPKTP crystal had been heated to 125°C to create an idler around 3.62 μm. The pump beam from the beam splitter (BS) enters the PPKTP with energy of 340 μJ. The output idler beam from the first stage was used as the signal beam for the second stage. A diffusion-bonded PPSLT crystal, with a period of 22.8 μm and aperture of 5.52 mm(H) × 9.53 mm(W), was heated to about 170°C and was used for the second amplification stage, where both the pump and signal beams were collimated to a diameter of 1.3 mm. Here, the second pumping beam has the energy of 715 μJ. The germanium filter was used to block the redundant wavelengths that were generated due to amplified spontaneous emission (ASE) in the PPKTP in order to not amplify an unwanted signal in the second stage. To capture the signal and idler beam profiles after the second OPCPA stage, different filters were used to select the desired wavelength (signal around 3.62 μm or 1.04 μm). A Si-based CCD camera and a motorized three-axis scanning photodiode were used as the detector to characterize the output beam profiles in the near-IR and mid-IR spectral range, respectively.

Figure 4 shows the beam profile of the amplified signal (3620 nm) and idler (1043 nm) outputs from the diffusion-bonded PPSLT. To determine the effects of stitching, we first shifted the pump and the signal beam off the crystal center in such a way that they went through only one crystal, and captured the beam profiles of both the signal and the idler [Figs. 4(a) and 4(b)]. Next, we moved them to the center of

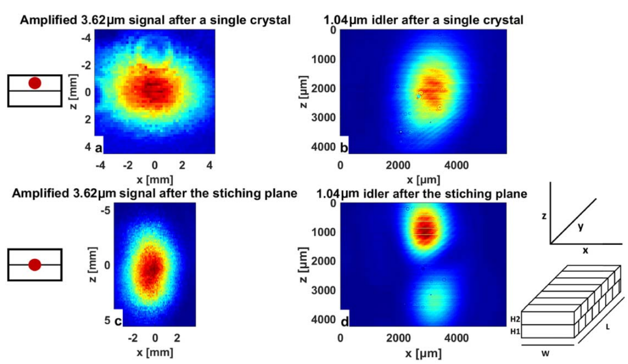

Fig. 4. Beam profile of the amplified signal (left) and idler (right) after the second stage of OPA. The inset to the bottom right shows schematic orientation of the stitched crystals. The two crystals are poled along the z axis and modulated along the y axis. The stitching plane (bonded area) is at the x–y plane. The beam propagation direction is along the y axis through the bonded crystal aperture at the x–z plane. The upper images are related to beams that were amplified in a single crystal, while the lower images are related to beams that overlap and are amplified by the two stitched crystals. It shows that the signal preserved its shape in both cases while the idler breaks into two lobes when overlapping the two bonded crystals. The created idler between the two diffusion-bonded crystals in our OPA has a similar profile to the simulation shown in Fig. 2.

the stitched crystals and made sure that the bonded surfaces were exactly in the middle of the pump and the signal beams and observed again the two beam profiles. The signal beam was scanned with a photodiode using pinholes of 200 μm diameter [Fig. 4(a)] and 100 μm [Fig. 4(c)] diameter, positioned on a motorized x–z stage. The idler beam profile was observed with a Si-based CCD camera. Figures 4(a) and 4(b) show the signal and the idler when they were amplified by only one crystal. They both show symmetrical beams. Figures 4(c) and 4(d) show the signal and the idler when the beams overlapped the two stitched crystals. While the signal beam [Fig. 4(c)] remained symmetrical, it was clear that the idler beam [Fig. 4(d)] broke into two separated lobes, which is the result of the relative phase between the two crystals. The created idler between the two diffusion-bonded crystals in our OPA [Fig. 4(d)] has a similar profile to a simulation shown in Fig. 2. Besides this effect, we observed some induced ellipticity of the signal beam. To make sure this ellipticity and the idler breakup were not coming from other effects such as noncollinear propagation or due to Fresnel reflection from the bonded interfaces, we made the following tests. First, we checked the collinear propagation for each individual crystal by just shifting laterally from one crystal to the other while keeping the pump and signal beam with the same alignment. We found that all beams keep propagating collinearly. Next, to test if we have Fresnel reflections from the bonded interfaces, we directed a He–Ne laser beam through the stitched crystal and did not see the two lobes presented above. The reasons for this ellipticity remained unclear, and extra investigation is needed. Despite this ellipticity, the beam can be used in future experiments. This result indicated that it is possible to combine several periodically poled crystals and to pump with higher energy (within a larger cross section) for the amplification of a signal in the OPA configuration.

In summary, we increased the width of a periodically poled crystal by stitching two crystals together using the diffusion-bonding technique. In previous work, a concern was raised that some residual misalignment between the domains of two stitched periodically poled crystals would potentially cause a deterioration in the beam profile, and may even break it into an asymmetrical beam. We discussed the likely cause for such deterioration in the beam shape due to an induced phase between the two sides of the output beam. We claim, and have experimentally demonstrated, that once the phases of both the pump and the signal are well predefined, only the phase of the idler will be affected by the domain misalignment and only the idler beam profile will be distorted while the amplified signal beam profile maintains a good quality. We conclude that diffusion bonding is a promising avenue towards large-aperture OPAs based on periodically poled crystals and will permit their use in high-energy applications.

Funding. Wolfson Foundation.

REFERENCES

1. C. Manzoni and G. Cerullo, J. Opt. **18**, 103501 (2016).
2. G. Cerullo and S. De Silvestri, Rev. Sci. Instrum. **74**, 1 (2003).
3. J. A. Armstrong, N. Bloembergen, J. Ducuing, and P. S. Pershan, Phys. Rev. **127**, 1918 (1962).
4. D. S. Hum and M. M. Fejer, C. R. Physique **8**, 180 (2007).
5. M. M. Fejer, G. A. Magel, D. H. Jundt, and R. L. Byer, IEEE J. Quantum Electron. **28**, 2631 (1992).
6. L. E. Myers, R. C. Eckardt, M. M. Fejer, R. L. Byer, W. R. Bosenberg, and J. W. Pierce, J. Opt. Soc. Am. B **12**, 2102 (1995).
7. G. Marcus, A. Zigler, D. Eger, A. Bruner, and A. Englander, J. Opt. Soc. Am. B **22**, 620 (2005).
8. G. Marcus, A. Zigler, A. Englander, M. Katz, and Y. Ehrlich, Appl. Phys. Lett. **82**, 164 (2003).
9. X. Gu, G. Marcus, Y. Deng, T. Metzger, C. Teisset, N. Ishii, T. Fuji, A. Baltuska, R. Butkus, V. Pervak, H. Ishizuki, T. Taira, T. Kobayashi, R. Kienberger, and F. Krausz, Opt. Express **17**, 62 (2009).
10. Y. Deng, A. Schwarz, H. Fattahi, M. Ueffing, X. Gu, M. Ossiander, T. Metzger, V. Pervak, H. Ishizuki, T. Taira, T. Kobayashi, G. Marcus, F. Krausz, R. Kienberger, and N. Karpowicz, Opt. Lett. **37**, 4973 (2012).
11. A. Zukauskas, N. Thilmann, V. Pasiskevicius, F. Laurell, and C. Canalias, Opt. Mater. Express **1**, 201 (2011).
12. G. Michaeli and A. Arie, Appl. Phys. B **77**, 497 (2003).
13. M. Peltz, U. Bäder, A. Borsutzky, R. Wallenstein, J. Hellström, H. Karlsson, V. Pasiskevicius, and F. Laurell, Appl. Phys. B **73**, 663 (2001).
14. F. Bach, M. Mero, M. H. Chou, and V. Petrov, Opt. Mater. Express **7**, 240 (2017).
15. J. L. Casson, K. T. Gahagan, D. A. Scrymgeour, R. K. Jain, J. M. Robinson, V. Gopalan, and R. K. Sander, J. Opt. Soc. Am. B **21**, 1948 (2004).
16. H. Ishizuki and T. Taira, Opt. Express **18**, 253 (2009).
17. S. Ganesamoorthy, M. Nakamura, S. Takekawa, S. Kumaragurubaran, K. Terabe, and K. Kitamura, Mater. Sci. Eng. B **120**, 125 (2005).
18. D. Chuchumishev, A. Gaydardzhiev, T. Fiebig, and I. Buchvarov, in *Lasers, Sources, and Related Photonic Devices*, OSA Technical Digest (CD) (Optical Society of America, 2012), paper AW4A.25.
19. H. Ishizuki and T. Taira, Opt. Lett. **30**, 2918 (2005).
20. H. Ishizuki and T. Taira, Opt. Express **20**, 20002 (2012).
21. K. Tei, M. Kato, F. Matsuoka, Y. Niwa, Y. Maruyama, T. Matoba, and T. Arisawa, Jpn. J. Appl. Phys. **38**, L35 (1999).
22. M. J. Missey, V. Dominic, L. E. Myers, and R. C. Eckardt, Opt. Lett. **23**, 664 (1998).
23. R. W. Boyd, *Nonlinear Optics*, 3rd ed. (Academic, 2008).
24. B. Dayan, A. Pe'er, A. A. Friesem, and Y. Silberberg, Phys. Rev. Lett. **93**, 023005 (2004).